

Supporting Information

Flexible, superhydrophobic and multifunctional carbon nanofiber hybrid membranes for high performance light driven actuators

Xin Song ^{a,b}, Xuewu Huang ^b, Junchen Luo ^b, Biao Long ^b, Weimiao Zhang ^b, Ling Wang ^b, Jiefeng Gao^{*b,c,d}, Huaiguo Xue^{*b}

^a Guangling College, Yangzhou University, Yangzhou, Jiangsu 225009, P. R. China

^b School of Chemistry and Chemical Engineering, Yangzhou University, Yangzhou, Jiangsu, 225002, P. R. China

^c State Key Laboratory of Polymer Materials Engineering, Sichuan University, Chengdu, Sichuan 610065, P. R. China.

^d Key Laboratory of Organosilicon Chemistry and Material Technology of Ministry of Education, Hangzhou Normal University, Hangzhou 311121, People's Republic of China

*Corresponding authors: jfgao@yzu.edu.cn;

Electromagnetic shielding performance measurement

The electromagnetic interference (EMI) shielding performance of the hybrid membranes was characterized by an Agilent Model N5230A vector network analyzer in X-band (8.2-12.4 GHz). The as-prepared membranes were cut into circular plates with a diameter of 15 mm, and an electromagnetic wave was guided into the samples by using the coaxial line technique. The measured scattering parameters (S11 and S21) were employed to calculate the EMI SE according to the following formula:

$$R = |S_{11}|^2$$

$$T = |S_{21}|^2$$

$$R + A + T = 1$$

$$\text{SET(dB)} = -10 \log T$$

$$\text{SER(dB)} = -10 \log(1 - R)$$

$$\begin{aligned} \text{SEA(dB)} &= \text{SE}_T - \text{SER} - \text{SEM} \\ &= -10 \log(T/1 - R) \end{aligned}$$

The total shielding (SE_T) is mainly caused by the sum of the contribution of absorption (SE_A), reflection (SE_R) and multiple reflection (SE_M), where SE_M can be ignored when $\text{SE}_T \geq 15$ dB.

Thermal conductivity testing

The thermal conductivity of the CNF hybrid membrane was tested by a laser flash technique (LFA 457 MicroFlash, Netzsch) and calculated according to the following formula:

$$K = \rho C_p \sigma$$

where ρ is the density of the CNF hybrid membrane, C_p is the specific heat which is measured through a method of sapphire with differential scanning calorimetry (DCS 8500), and σ is thermal diffusivity.

Photothermal performance of the CNF hybrid membrane

The photothermal conversion efficiency (η) of the CNF hybrid membrane was determined from the following equation¹.

$$\eta = \frac{hA\Delta T_{max}}{I(1 - 10^{-A_{808}})}$$

Where h represents the heat transfer coefficient, A represents the surface area of the system, ΔT_{max} (80.9 °C) represents the maximum temperature change, I represents the laser power (0.2 W) and A_{808} is the absorbance of the samples at the wavelength of 808 nm (0.95). In order to obtain the value of hA , θ is introduced as follows:

$$\theta = \frac{T - T_{surr}}{T_{max} - T_{surr}}$$

where T is the temperature of the CNF hybrid membrane, T_{max} is the maximum system temperature, and T_{surr} is the initial temperature. The θ and t are introduced to establish a functional relationship:

$$t = -\frac{\sum m_i c_{p,i}}{hA} \ln \theta$$

Where m (1.4 mg) and c_p ($2.049 \text{ J (g } ^\circ\text{C)}^{-1}$) are the weight and specific heat of system components (CNF hybrid membrane), respectively. Therefore, hA can be acquired from the time of cooling period vs θ . the photothermal conversion efficiency (η) of CNF hybrid membrane can be calculated.

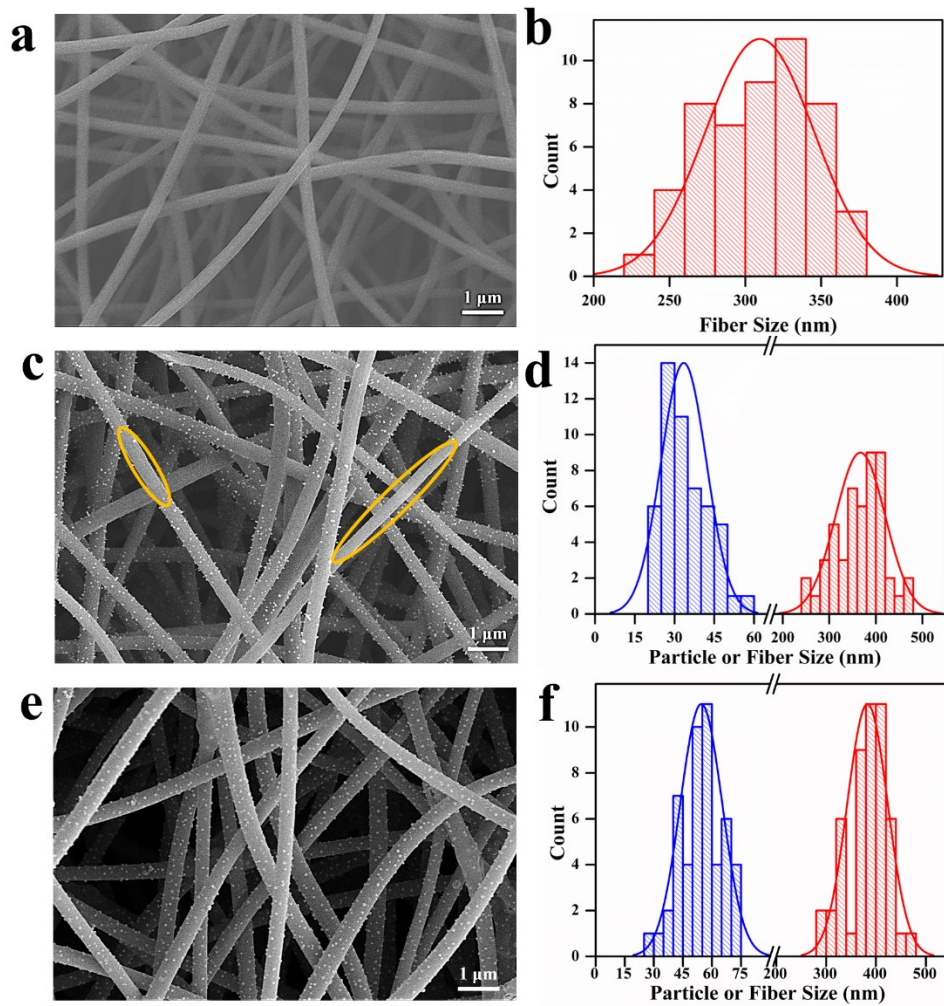


Fig. S1 SEM images of the carbon nanofibers and the statistical diameter distributions.

(a-b) CNF. (c-d) CNF-Ni1. (e-f) CNF-Ni2.

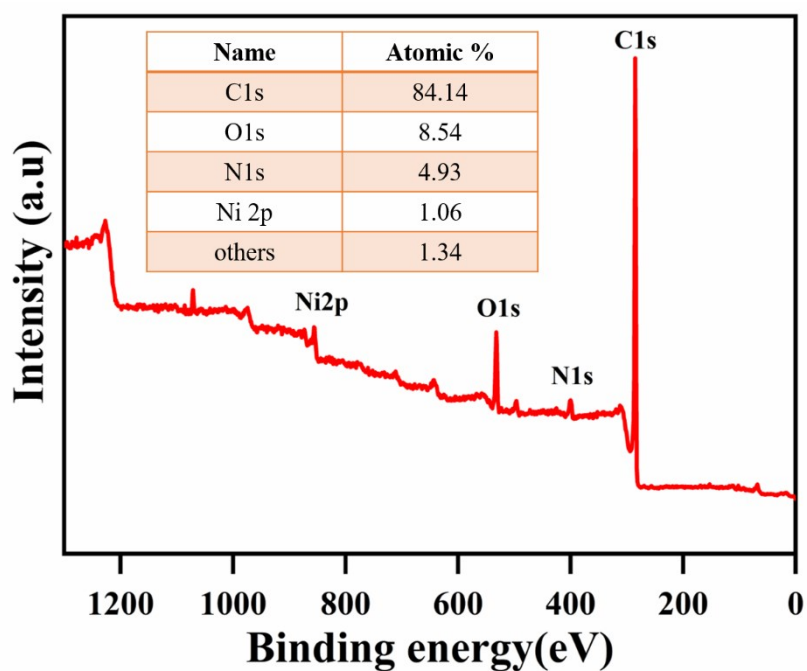


Fig. S2 The XPS spectrum of CNF-Ni2 and the content ratio of corresponding atoms.

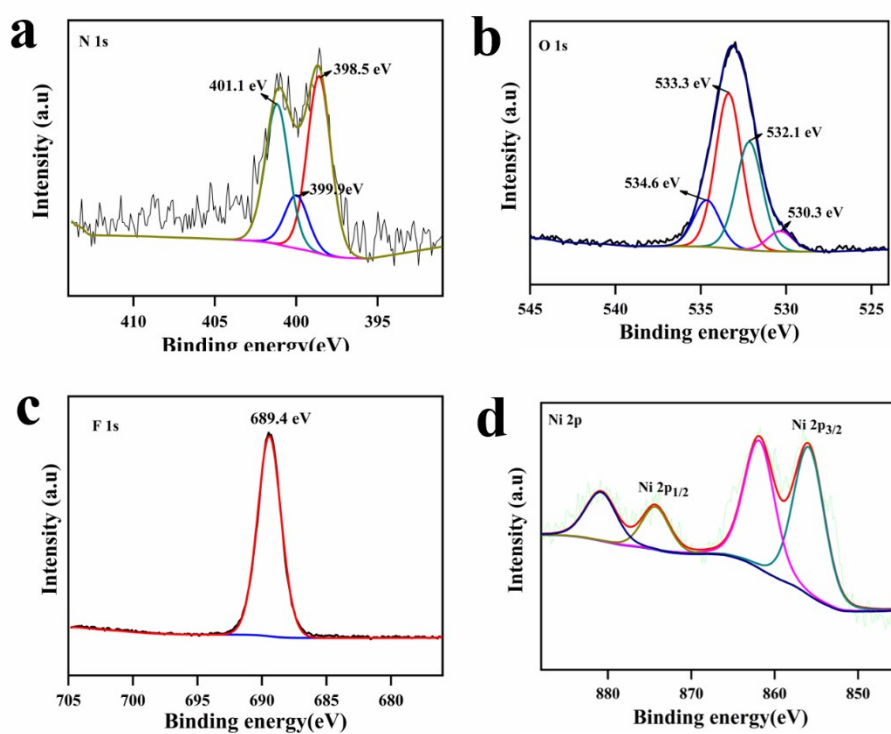


Fig. S3 The XPS spectrum of CNF-Ni2-F: (a) N 1s peak fitting; (b) O 1s peak fitting; (c) F 1s peak fitting; (d) Ni 2p peak fitting.

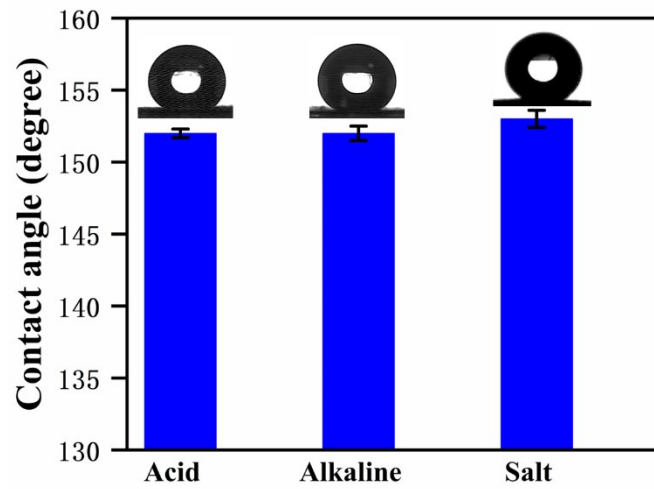


Fig. S4 the CAs of the composite membranes after immersion into acid (pH=3), alkaline (pH=14) and salt conditions for 3 h.

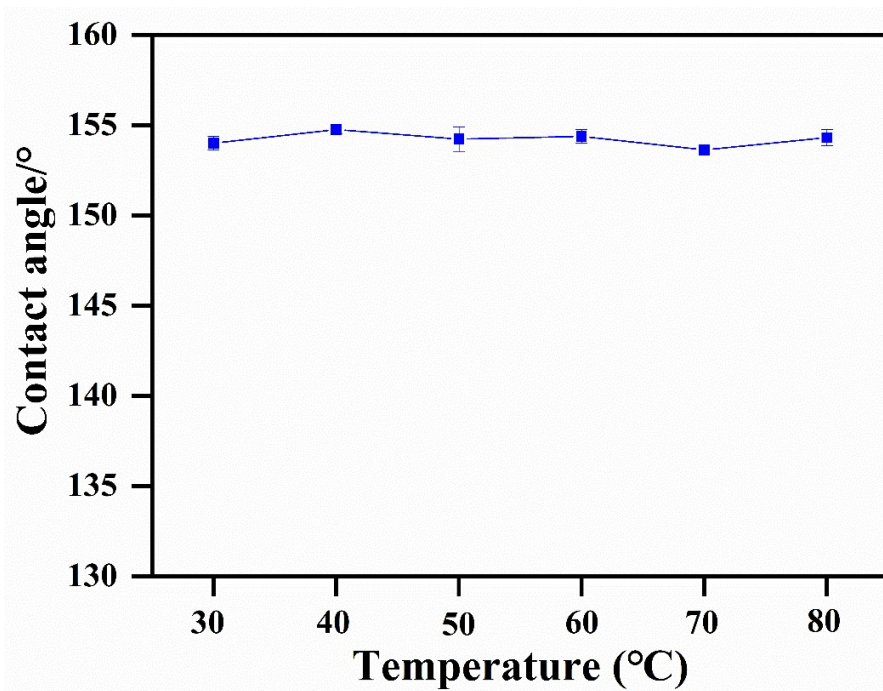


Fig. S5 CAs on the superhydrophobic membrane surface as a function of the temperature.

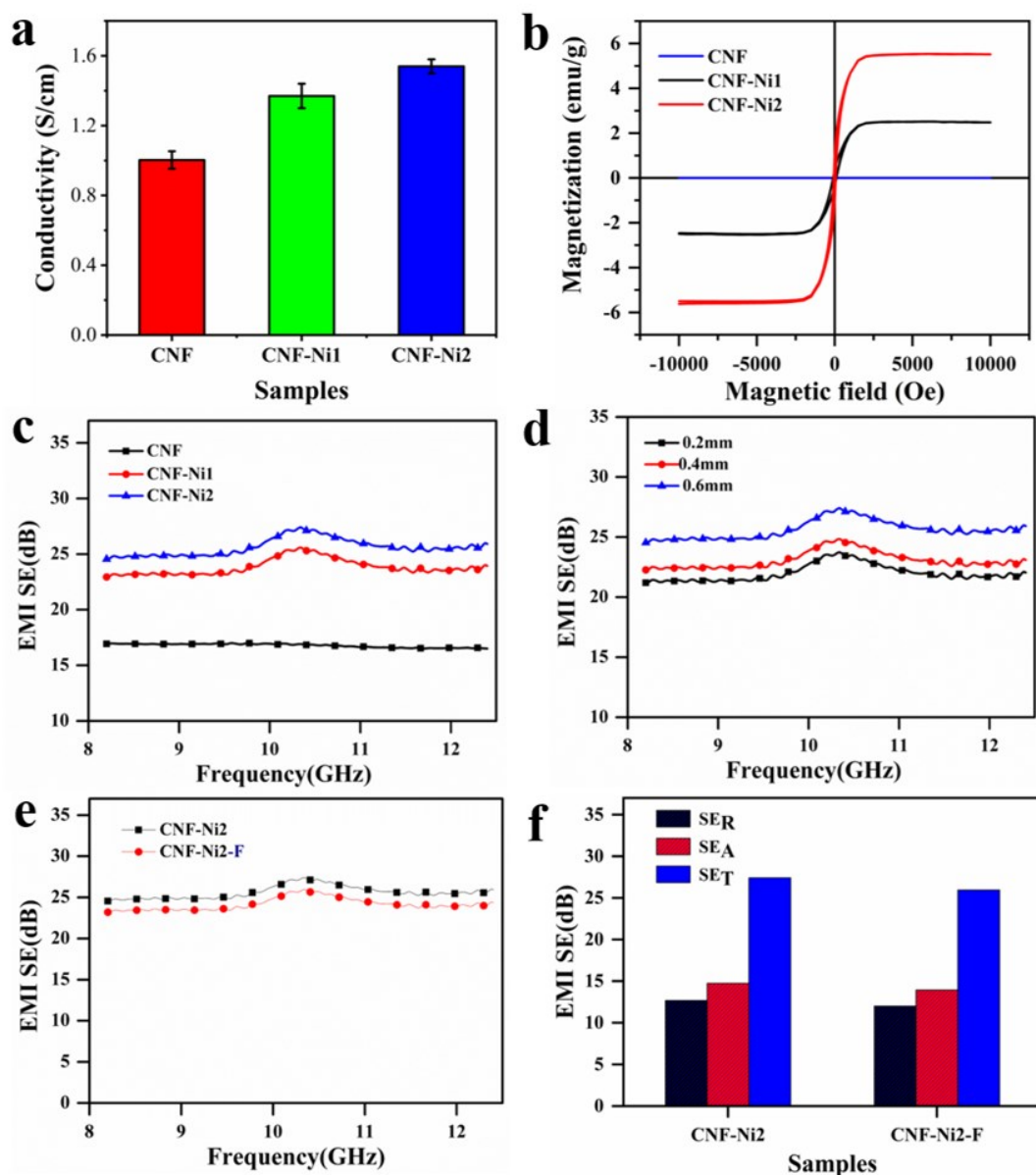


Fig. S6 (a) Electrical conductivity and (b) magnetic hysteresis loops of the CNF, CNF-Ni1 and CNF-Ni2 membrane. (c) Variation in shielding effectiveness with frequency (8.2-12.4 GHz) for CNF and its hybrid membranes. (d) EMI shielding effectiveness of the CNF-Ni2 in the X band with different thickness. (e and f) Comparison of the EMI SE of the CNF-Ni2 samples (with a thickness of about 0.6 mm) before and after fluorination.

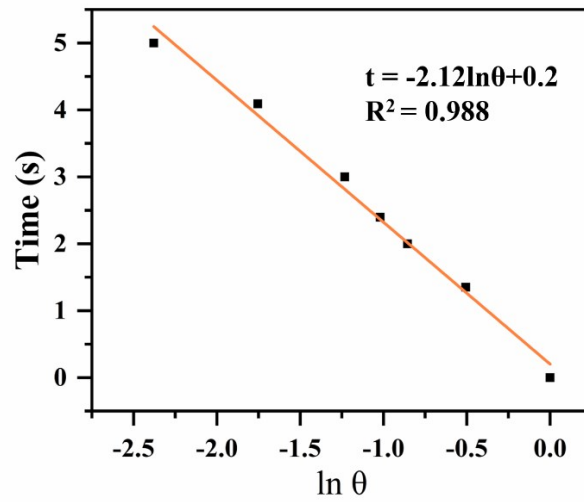


Fig. S7 A linear fitting correlation between time (t) and $\ln \theta$ from the cooling period.

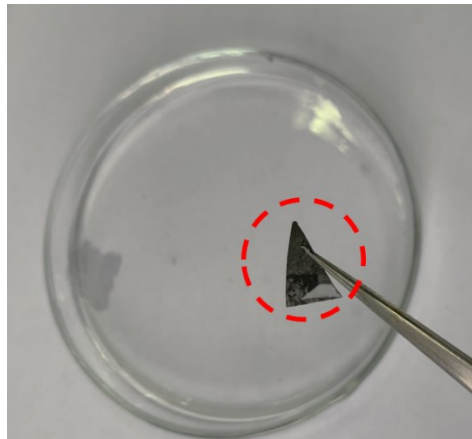


Fig. S8 Photograph of the CNF-Ni₂ membrane wetted by water after.

Table S1 Comparison of EMI shielding performance of various carbon nanomaterials

Sample	Thickness (mm)	Density (g/cm ³)	EMI SE (dB)	SSE (dB cm ³ g ⁻¹)	Ref.
PP/MWCNT coated PET fabrics	1.65	0.2236	20	89.44	2
Activated Carbon Web	11.6	2.78	75.44	27.14	3
MWCNT-Dip-Coated Cotton Fabrics	0.5	0.29	11.48	39.6	4
CF/PC/Ni film	0.31	1.7	72.7	42.76	5
CNT/carbon fiber/pyrolytic carbon	2	0.93	72.8	78.3	6
MCMBs/MWCNTs/Fe ₃ O ₄	0.5	0.5	80	160	7
This work	0.6	0.142	26	/	183.1

Table S2. Comparison of the photothermal efficiency (η) among various carbon nanomaterials.

Materials	Laser power (W)	η (%)	Ref.
Oxidized mesoporous carbon Nanoparticles	2	27.4	8
glucose-derived carbonaceous nanospheres	2	35.1	9
MoS ₂ @C nanocomposite	1.67	40.8	10
Graphite	1	34.2	
Graphitic carbon nanocubes	0.5	40.4	11
This work	0.2	61.6	

References

1. Wang, Y., Guo, Q. Q., Su, G. H., Cao, J., Liu, J. Z., Zhang, X. X., Hierarchically Structured Self-Healing Actuators with Superfast Light- and Magnetic-Response. *Adv. Funct. Mater.* **2019**, 29(50), 1906198.
2. Lin, Z.-L., Lou, C.-W., Pan, Y.-J., Hsieh, C.-T., Huang, C.-H., Huang, C.-L., Chen, Y.-S., Lin, J.-H., Conductive fabrics made of polypropylene/multi-walled carbon nanotube coated polyester yarns: Mechanical properties and electromagnetic interference shielding effectiveness. *Compos. Sci. Technol.* **2017**, 14174.
3. Naeem, S., Baheti, V., Tunakova, V., Militky, J., Karthik, D., Tomkova, B., Development of porous and electrically conductive activated carbon web for effective EMI shielding applications. *Carbon* **2017**, 111439.
4. Zou, L. H., Yao, L., Ma, Y., Li, X. P., Sailimujiang, S., Qiu, Y. P., Comparison of polyelectrolyte and sodium dodecyl benzene sulfonate as dispersants for multiwalled carbon nanotubes on cotton fabrics for electromagnetic interference shielding. *J. Appl. Polym. Sci.* **2014**, 131(15).
5. Xing, D., Lu, L. S., Teh, K. S., Wan, Z. P., Xie, Y. X., Tang, Y., Highly flexible and ultra-thin Ni-plated carbon-fabric/polycarbonate film for enhanced electromagnetic interference shielding. *Carbon* **2018**, 13232.
6. Liu, X. M., Yin, X. W., Kong, L., Li, Q., Liu, Y., Duan, W. Y., Zhang, L. T., Cheng, L. F., Fabrication and electromagnetic interference shielding effectiveness of carbon nanotube reinforced carbon fiber/pyrolytic carbon composites. *Carbon* **2014**, 68501.
7. Chaudhary, A., Kumar, R., Teotia, S., Dhawan, S. K., Dhakate, S. R., Kumari, S.,

Integration of MCMBs/MWCNTs with Fe₃O₄ in a flexible and light weight composite paper for promising EMI shielding applications. *J. Mater. Chem. C* **2017**, 5(2), 322.

8. Wang, X., Li, X., Mao, Y., Wang, D., Zhao, Q., Wang, S., Multi-stimuli responsive nanosystem modified by tumor-targeted carbon dots for chemophototherapy synergistic therapy. *J. Colloid. Interface Sci.* **2019**, 552639.

9. Miao, Z. H., Wang, H., Yang, H., Li, Z., Zhen, L., Xu, C. Y., Glucose-Derived Carbonaceous Nanospheres for Photoacoustic Imaging and Photothermal Therapy. *ACS Appl. Mater. Interfaces* **2016**, 8(25), 15904.

10. Zhang, X., Zhao, Z., Yang, P., Liu, W., Fan, J., Zhang, B., Yin, S., MoS₂@C nanosphere as near infrared / pH dual response platform for chemical photothermal combination treatment. *Colloids Surf. B.* **2020**, 192111054.

11. Chen, W., Zhang, X., Ai, F., Yang, X., Zhu, G., Wang, F., Graphitic Carbon Nanocubes Derived from ZIF-8 for Photothermal Therapy. *Inorg. Chem.* **2016**, 55(12), 5750.